ACS Catalysis

Research Article

pubs.acs.org/acscatalysis

Elucidating the Roles of Zeolite H-BEA in Aqueous-Phase Fructose Dehydration and HMF Rehydration

Jacob S. Kruger, Vinit Choudhary, Vladimiros Nikolakis,* and Dionisios G. Vlachos*

Catalysis Center for Energy Innovation, Department of Chemical and Biomolecular Engineering University of Delaware, 150 Academy Street, Newark, Delaware 19716, United States

Supporting Information

ABSTRACT: The main paths by which zeolites carry out the dehydration of fructose to HMF and the rehydration of HMF to levulinic acid in aqueous solutions are elucidated using an H-BEA zeolite with SiO_2/Al_2O_3 = 18 (H-BEA-18) as a representative solid acid catalyst. Specifically, the relative role of homogeneous chemistry (both solvent- and zeolite-induced), the effect of external surface acid sites, and the effect of adsorption of products and reactants on the catalyst for these reactions is delineated. We found that H-BEA-18 increases the conversion of fructose and HMF in part by catalyzing fructose isomerization to glucose and HMF rehydration to formic and levulinic acids, respectively. The glucose-to-fructose isomerization is caused by octahedral aluminum atoms that act as Lewis acid sites as shown by ^{1}H and ^{13}C NMR. These Lewis sites are formed during calcination and are stable under reaction conditions. They also catalyze reactions to unknown products from both fructose and HMF. The acids produced from HMF rehydration dissolve aluminosilicate species from the zeolite, which also catalyze some of the undesired side reactions. We show that the decrease of the initial pH due to the addition of the zeolite and the catalysis by sites on the external surface of the zeolite have a negligible contribution to the chemistry under most conditions investigated. H-BEA-18 more readily converts HMF than fructose, due to strong preferential adsorption of HMF, furfural, and levulinic acid compared to sugars. Under mildly acidic conditions (without the addition of inorganic acids) that are environmentally preferred, zeolites can increase the conversion of HMF and the selectivity to levulinic acid many-fold. This provides an indication that heterogeneous materials may be superior in the production of levulinic acid from HMF.

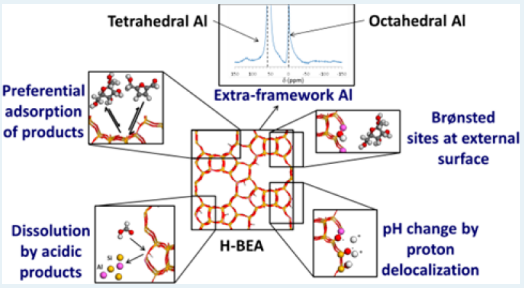

KEYWORDS: *aqueous phase, dehydration, rehydration, fructose, glucose, HMF, levulinic acid, BEA zeolite, adsorption, zeolite stability*

1. INTRODUCTION

Reactions producing 5-hydroxymethyl furfural (HMF) and levulinic acid from sugar molecules represent important steps in the conversion of biomass to chemicals and fuels.[1] In general, hydrolysis of C_6 carbohydrate polymers (e.g., starch, cellulose, inulin, etc.) produces glucose and fructose monomers, the latter of which can undergo three sequential dehydration reactions to produce HMF. HMF can be rehydrated to produce levulinic acid (with concomitant generation of an equimolar portion of formic acid) as shown in Scheme 1. Under certain conditions, HMF can also be oxidized to furandicarboxylic acid (FDCA) or produce other valuable intermediates in a renewable chemicals industry.[2] In each step, sugars and furans can also react to undesired side products through fragmentation (e.g., producing lactic acid or glycolaldehyde) or polymerization reactions to produce insoluble humins and soluble humin precursors.

The dehydration of fructose to HMF has been studied using a variety of solvent and catalyst combinations. The aim of these studies was either to maximize the HMF yield or to gain insight into the dehydration chemistry, and the main findings are summarized in several recent reviews.[3−9] Zeolite catalysts may offer advantages over other acidic catalysts in sugar dehydration, including simple catalyst separation relative to homogeneous acid catalysts, stability in high-temperature aqueous systems compared to other materials, such as Amberlyst resins, and stability to thermal regeneration.[10] Indeed, zeolite catalysts have frequently been investigated for glucose and fructose dehydration reactions,[10−17] and significant effort has gone into developing shape selective catalysts for sugar dehydration.[18−29] We recently reviewed the literature on these catalysts and proposed that catalyst properties (e.g., Brønsted/Lewis acidity and hydrophobicity) and reaction conditions (e.g., solvent choice) interact in complex ways to alter yields to desired products. This complex interplay of process conditions, substrate, and catalyst properties has precluded a fundamental understanding of the roles of zeolites in sugar dehydration.[30]

In this work, we propose a methodology of simple yet robust experiments to cope with the complexity of these systems and delineate the pathways by which many solid acid catalysts influence sugar dehydration and HMF rehydration chemistry. This mechanistic understanding can help us design better

Received: March 20, 2013
Revised: April 28, 2013
Published: April 30, 2013

   dx.doi.org/10.1021/cs4002157 | ACS Catal. 2013, 3, 1279−1291

Scheme 1. Simplified Reaction Network for Dehydration of Fructose to HMF and Rehydration of HMF to Formic and Levulinic Acids

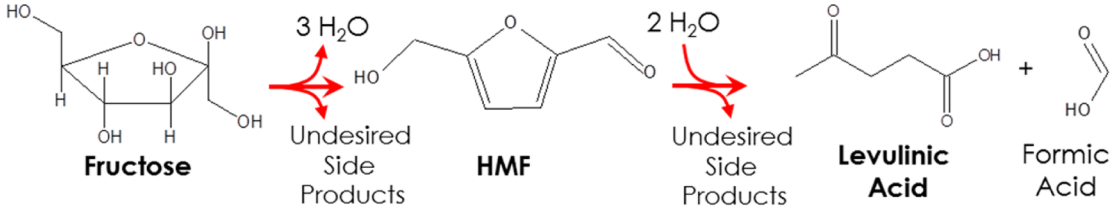

catalysts. We used an H-BEA zeolite catalyst with Brønsted acidity as a representative catalyst. We are interested in exploring the BEA zeolite framework in relation to the Sn-BEA zeolite, a Lewis-acid zeolite that is highly active and selective for glucose isomerization under similar reaction conditions. In particular, we are motivated by the possibility of synthesizing a bifunctional H(Al)/Sn-BEA zeolite catalyst to combine both Brønsted and Lewis functionalities in a single catalyst. According to the International Zeolite Association database, zeolite BEA has a three-dimensional pore network with 6.6 × 6.7 Å and 5.6 × 5.6 Å channels.

We investigate five mechanisms to rationalize the zeolite catalyst performance, as shown in Scheme 2. First, preferential adsorption of products on the zeolite can alter apparent selectivity to strongly adsorbed products, as measured from products in solution, and may result in further reaction of these products. Second, aluminum or silicon species may be dissolved by acidic reaction products, such as formic acid, and act as homogeneous catalysts. Third, the zeolite may induce homogeneous acid catalysis through dissociation of Brønsted sites or weak-acid silanol groups, which cause a decrease in initial solution pH. We report the contribution of homogeneous chemistry to the observed product distribution, which is often significant under reaction conditions, but not commonly considered. Fourth, reactions catalyzed by Brønsted sites on the external catalyst surface may exhibit different selectivity than in-pore reactions due to lack of confinement. We approach these mechanisms with a series of experiments comparing catalyst loading, catalyst properties (framework structure and surface passivation), solvent properties (pH and acid type), and postreaction analysis of catalysts and solvents.

Scheme 2. Potential Mechanisms by Which the Zeolite Can Influence Sugar Dehydration Selectivity

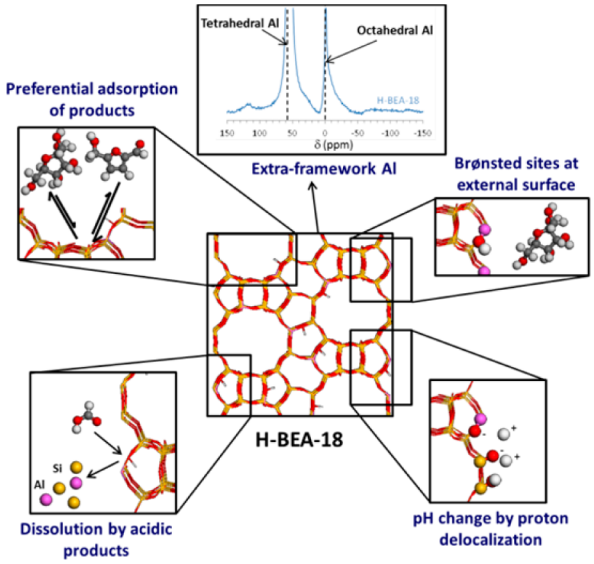

2. MATERIALS AND METHODS

2.1. Materials and Catalyst Preparation. Fructose (BioXtra, ≥ 99%), glucose (BioUltra, ≥ 99.5%), HMF (≥99%), formic acid (Fluka, 98%), levulinic acid (98%), furfural (98%), hydrochloric acid (1.0 M), and tetraethyl orthosilicate (98%) were purchased from Sigma Aldrich. Glucose labeled with deuterium at the C2 position (glucose-D-2, 98%) was purchased from Cambridge Isotope Laboratories, and BEA zeolite with a SiO_2/Al_2O_3 ratio = 18 (BEA-18) was purchased from Zeolyst in the ammonium form. To generate the acidic form of the zeolite, ammonium-form zeolite (NH_4−BEA−18) was calcined in ambient air with the following temperature program: ramp temperature at 2 °C/min to 90 °C, hold for 1 h, ramp at 2 °C/min to 450 °C, hold for 8 h, cool to room temperature. We denote the resulting acidic form as H-BEA-18.

In some experiments, the surface of the H-BEA-18 catalyst was passivated by coating the zeolite with a layer of SiO_2 by a procedure similar to that of Weber et al.[31] Briefly, the zeolite was suspended in a 5 vol % mixture of tetraethyl orthosilicate (TEOS) in hexane (2.5 g zeolite in 20 mL solution), stirred at room temperature for 24 h, filtered, and calcined as above to generate the SiO_2 layer.

2.2. Reaction Procedure. Reactors consisted of 5 mL conical screw-cap glass vials from Chemglass, fitted with a triangular magnetic stir vane and sealed with a PTFE/polypropylene septum. Experiments were performed at 130 °C, using aqueous solutions of 10 wt % fructose, 10 wt % glucose, 0.25 wt % HMF, 0.1 wt % levulinic acid, or 0.027 wt % furfural. These concentrations of HMF, levulinic acid, and furfural were selected to match the highest concentrations observed using 10 wt % fructose as the reagent. The solution was pipetted into the glass reaction vials, maintaining approximately constant headspace (3.45 g solution per vial). H-BEA-18 was added to the vial to give the desired aluminum-to-fructose molar ratio (Al/Fru), and the pH of the resulting mixture was measured. The Al/Fru ratios explored were 0, 0.03, 0.10, and 0.30, corresponding to fructose-to-zeolite mass ratios of ∞ (no zeolite), 10, 3, and 1, respectively. A magnetic stir bar was added, and the vials were sealed and weighed. Vials were added to preheated oil-filled wells in an aluminum block on a hot plate stirrer at 130 °C and a timer started as soon as the vials were in the oil bath. Reaction temperature was typically reached within 5 min and was monitored throughout the reaction by a thermocouple placed inside an oil-filled vial in the block. Vials were removed periodically, quenched in water, cleaned of oil residue on their external surface, and weighed to 0.1 mg precision to ensure their mass had not decreased during

dx.doi.org/10.1021/cs4002157 | ACS Catal. 2013, 3, 1279−1291

Scheme 3. Flow Chart Representation of Zeolite Filtrate (ZF) and pH = 3 Formic Acid Experiments

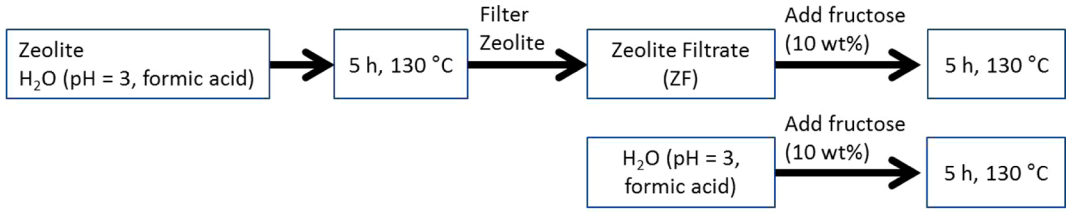

Table 1. Conditions of Experiments Carried out in This Study[a]

run	feed	solvent	catalyst	Al/Fru molar ratio	initial pH	final pH[b]
1	10 wt % fructose	H_2O	none	0	5.40	2.74
2		H_2O	H-BEA-18	0.03	4.31	3.13
3		H_2O	H-BEA-18	0.10	4.25	3.14
4		H_2O	H-BEA-18	0.30	4.07	2.96
5		H_2O	TEOS-H-BEA-18	0.10	4.68	2.94
6		H-BEA-18 ZF	formic acid	1.4×10^{-3}	3.34	2.71
7		MIBK/H_2O = 3	H-BEA-18	0.10	3.86	3.56
8		H_2O	HCl-H-BEA-18	ND	3.74	2.52
9		MIBK/H_2O = 3	HCl-H-BEA-18	ND	4.41	2.87
10		H_2O	HCl	0	3.03	2.99
11		H-BEA-18 ZF	HCl	6.0×10^{-5}	3.68	2.77
12		H_2O	HCl	0	3.97	2.80
13	10 wt % glucose	H_2O	none	0	5.42	3.20
14		H_2O	H-BEA-18	0.10[c]	4.06	3.27
15		H_2O	TEOS-H-BEA-18	0.10[c]	4.61	3.56
16	0.25 wt % HMF	H_2O	none	0	4.92	3.24
17		H_2O	HCl	0	3.93	2.99
18		H_2O	H-BEA-18	0[d]	4.39	3.56
19	0.027 wt % furfural	H_2O	none	0	4.61	4.45
20		H_2O	H-BEA-18	0[d]	4.31	4.12
21	0.1 wt % levulinic acid	H_2O	none	0	3.34	3.38
22		H_2O	H-BEA-18	0[d]	3.93	3.84
23		H_2O	10 wt % fructose	0	3.42	3.12[e]
24		H_2O	0.25 wt % HMF	0	3.30	3.37[e]

[a]See Materials and Methods for abbreviations. Standard deviation of pH values is generally <0.10 pH units. [b]pH measured after ~5 h reaction time at 130 °C and cooling to room temperature. [c]Al/glucose molar ratio. [d]H-BEA-18 was loaded as if to give 10 wt % fructose Al/Fru = 0.10. [e]pH was measured after 1.25 h reaction time. TEOS-H-BEA-18 = H-BEA-18 with TEOS-passivated surface. HCl-H-BEA-18 = H-BEA-18 washed with HCl to remove extra-framework Al. ND = not determined.

the reaction. A final pH measurement was taken, and the reaction liquid was filtered through a 0.20 μm nylon syringe filter. Filtered solids were rinsed and dried by vacuum through Whatman No. 1 filter paper.

To generate zeolite filtrate and for reuse and biphasic experiments, a 125 mL stainless steel Parr reactor was used to facilitate catalyst recovery. In these experiments, 65 g of solution was employed, and the reactor required 30 min to reach reaction temperature. In these cases, the reaction time was started 25 min after heating began; in this configuration, conversion and selectivity after 5 h reaction time were within experimental error of those observed in the 5 mL glass vial reactors. In experiments employing an organic extracting phase, methyl isobutyl ketone (MIBK) was added in a 3:1 mass ratio (3.9:1 volume ratio) with the aqueous phase. Previous work has shown that the benefit of organic phase plateaus above a 3:1 volume ratio.[32]

Conversion, selectivity, and yield were calculated respectively as

$$X_{Fru} = \frac{[Fru]_0 - [Fru]_t}{[Fru]_0} \times 100\%$$

$$S_i = \frac{[i]_t n_{C_i}}{([Fru]_0 - [Fru]_t) n_{C_{Fru}}} \times 100\%$$

$$Y_i = \frac{[i]_t}{[Fru]_0} \times 100\%$$

where i denotes a species other than fructose, n_{C_i} is the number of carbon atoms in species i, *Fru* denotes fructose, subscript t denotes reaction time, subscript 0 denotes initial time (that is, t = 0), and terms in brackets are concentrations in mol/L.

dx.doi.org/10.1021/cs4002157 | ACS Catal. 2013, 3, 1279−1291

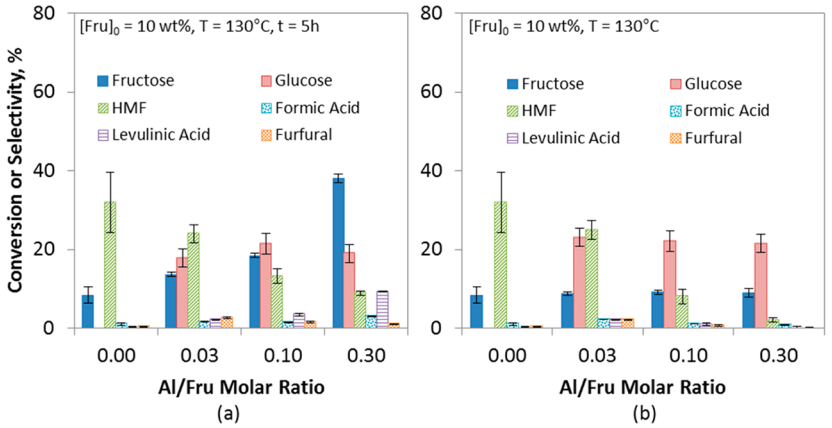

Figure 1. Conversion and selectivity data for 10 wt % aqueous fructose at 130 °C with different zeolite loadings (a) after 5 h of reaction time and (b) at 8% fructose conversion. Selectivity is on a carbon atom basis. Error bars represent the standard deviation of at least two replicates. Kinetic data for the entire duration are available in Figure S1. The homogeneous case corresponds to Al/Fru = 0.00.

In experiments with glucose-D-2, the initial concentration of glucose was 20 wt % (with Sn-BEA) or 25 wt % (with H-BEA-18), and the reaction temperature was 140 °C. For the H-BEA-18 catalyst, the glucose-to-zeolite mass ratio was three (Al/Glu = 0.1), and the reaction time was 3.5 h. For the Sn-BEA zeolite, the catalyst was synthesized as described elsewhere.[33] The glucose-to-zeolite mass ratio was 11.2 (Sn/Glu = 0.01), and the reaction time was 20 min. After reaction, the reaction mixture was analyzed via HPLC as described in section 2.5 below, except that the eluent fraction containing glucose and fructose was collected in test tubes by an automated fraction collector. The sugar fraction of several injections was collected and combined, concentrated by evaporation at 40 °C under vacuum, and rediluted with ~10% D_2O prior to NMR analysis.

2.3. Zeolite-Induced Homogeneous Reactions. In order to understand the effect of homogeneous chemistry induced by the acidity of the zeolite, three experiments were conducted. First, zeolite was suspended in water (atmosphere-equilibrated, pH ~5.6, or pH = 3, adjusted using formic acid or HCl), heated to the reaction temperature for 5 h, and filtered through a 0.2 μm filter. Fructose was added to the filtrate to produce a 10 wt % solution, and the homogeneous dehydration reaction was performed as above. This experiment is labeled as zeolite filtrate (ZF) and represented graphically in Scheme 3. Because the initial pH of the zeolite filtrate solution was lower than that of the original homogeneous experiment, 10 wt % fructose was also dehydrated in water with formic acid and HCl at an initial pH = 3 for comparison.

Additionally, the dehydration reaction was performed with 10 wt % fructose and 0.25 wt % HMF solutions with no zeolite added, but with the solution adjusted to an initial pH = 4 with HCl, which was the lowest initial pH observed in the experiments with zeolite. All experiments are summarized in Table 1.

2.4. Adsorption. The amount of fructose, glucose, HMF, formic acid, levulinic acid, and furfural adsorbed in H-BEA-18 at the end of the reaction was measured by resuspending postreaction H-BEA-18 from the highest catalyst loading (aluminum to fructose molar ratio, Al/Fru = 0.30) in 5 mL of deionized water, allowing the mixture to equilibrate for 24 h at room temperature, filtering the zeolite, and measuring the concentration of each analyte in the filtrate. This amount of water was chosen to provide adequate solution for resuspending the zeolite while ensuring that desorbed products were not too dilute to analyze. Adsorption on the nylon filter material was assumed to be negligible.

2.5. Analytical Methods. Reaction liquids were analyzed on a Waters 2695 HPLC system with 2414 Refractive Index and 2998 Photodiode Array (UV) Detectors. Analytes were separated on a BioRad Aminex HPX-87H column at 65 °C with 0.005 M H_2SO_4 mobile phase at 0.65 mL/min. For HPLC-MS/MS analysis, the same model column was used in an Agilent 1100 HPLC system with a 2000 QTRAP mass spectrometer from AB Sciex at a flow rate of 0.25 mL/min at room temperature with 0.1% formic acid (pH = 2.8) as the mobile phase.

The surface area of H-BEA-18 was measured via N_2 physisorption at 77 K on a Micromeritics ASAP 2020 Surface Area and Porosity Analyzer. XRD was performed on a Philips X'Pert X-ray diffractometer with a Cu Kα source, 45 kV tension, and 20 mA current. Scan step size was 0.01° with a dwell time of 2 s. Thermogravimetric Analysis (TGA) was performed on a Mettler-Toledo TGA/DSC1 thermal analyzer, equipped with a STAR^e system and a GC2000 gas controller. Samples were thoroughly rinsed with deionized water before TGA analysis. TGA was carried out with 150 μL Al_2O_3 sample cups and heating from 25 to 800 °C at 10 °C/min in dry air. Reaction and ZF solutions were analyzed using inductively coupled plasma (ICP) with a Thermo Elemental Intrepid II XSP Duo View ICP using the 167.0 and 308.2 nm spectral lines for Al and the 251.6 nm spectral line for Si.

Solid-state ^{27}Al Nuclear Magnetic Resonance (NMR) spectroscopy was performed on a Bruker AVIII 500 MHz spectrometer in single-pulse mode with a 4 mm HX MAS probe, 8 kHz spinning rate, 2048 scans, 0.5 s recycle delay time, and 1.0 μs pulse width, based on the method of Shetti et al.[34] Chemical shifts were referenced to 1 M aqueous $Al(NO_3)_3$. For ^{1}H and ^{13}C NMR, spectra were measured with a Bruker AV400 spectrometer in 90% H_2O/10% D_2O solvent using a 5 mm CPQNP probe and pulse widths of 9.25 and 15 μs for ^{13}C and ^{1}H spectra, respectively.

Brønsted acid site concentrations were measured via TGA of adsorbed isopropyl amine (IPA) with a SDT Q600 from TA Instrument as described previously.[35] Briefly, the sample was treated at 550 °C for 2 h under a dry helium flow before cooling to 120 °C and subsequently bubbling helium through liquid IPA prior to the catalyst chamber. Helium was bubbled until equilibrium was reached and then redirected to bypass the

dx.doi.org/10.1021/cs4002157 | ACS Catal. 2013, 3, 1279−1291

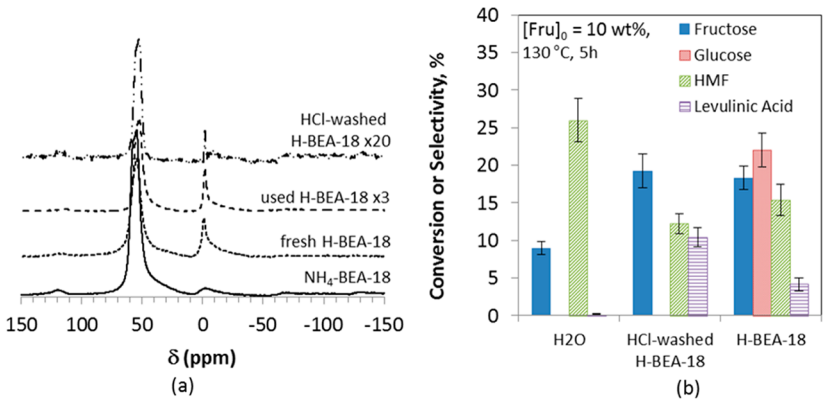

Figure 2. (a) ^{27}Al NMR of uncalcined NH_4−BEA-18, freshly calcined H-BEA-18, thrice-used H-BEA-18 after dehydration of 10 wt % fructose at 130 °C for 5 h each run, and H-BEA-18 after washing with HCl to remove octahedral Al. (b) Fructose conversion and selectivity to glucose, HMF, and levulinic acid in the homogeneous system, with HCl-washed H-BEA-18, and unwashed H-BEA-18.

bubbler. Redirected flow was maintained at 100 mL/min for ≥1 h to flush out weakly adsorbed IPA. Temperature-programmed desorption was then carried out with a heating rate of 10 °C/min to 700 °C. Brønsted acid site concentrations were calculated by the weight loss between 300 and 400 °C, the temperature range over which IPA decomposes.[36]

3. RESULTS AND DISCUSSION

3.1. Effect of Zeolite Loading on Product Distribution.

As an initial metric of zeolite activity and selectivity, we investigated fructose conversion and glucose, HMF, formic acid, levulinic acid, and furfural selectivity as a function of zeolite loading. Results after 5 h of reaction time at 130 °C are shown in Figure 1a; Figure 1b shows the selectivity at constant (∼8%) fructose conversion. The leftmost set of bars is in the absence of zeolite (homogeneous only chemistry). It is clear that under the same operating conditions, homogeneous chemistry can happen. It can be seen that fructose conversion and selectivity to formic acid and levulinic acid after a 5 h increase with increasing catalyst loading (increasing Al/Fru). The opposite is observed for the HMF selectivity, suggesting that the zeolite catalyzes the conversion of fructose and the rehydration of HMF to formic and levulinic acids, as expected. Selectivity to furfural, another desirable furanic product, is slightly higher in the presence of the zeolite. The contribution of heterogeneous acid chemistry to the dehydration increases over that of homogeneous chemistry with increasing catalyst loading, which is an expected result when both chemistries are active.

At ∼8% fructose conversion, HMF selectivity similarly decreases with increasing zeolite loading, but the trend for formic acid, levulinic acid, and furfural is nonmonotonous, peaking at Al/Fru = 0.03. This suggests that in addition to the rehydration of HMF, the zeolite also catalyzes side reactions of these products, leading to unidentified species that were not detected via HPLC.

In each case with H-BEA-18, glucose selectivity is 20−30%, whereas no glucose was observed without the zeolite. This result suggests that H-BEA-18 catalyzes the isomerization, probably due to the presence of Lewis acid sites that may arise from octahedral or extra-framework Al.[37] To examine whether the H-BEA-18 catalyst contained octahedral aluminum atoms, calcined H-BEA-18 and uncalcined NH_4−BEA were analyzed with ^{27}Al solid-state NMR. The analysis showed that the fresh NH_4−BEA-18 contains only one prominent resonance at ∼60 ppm, indicative of tetrahedral Al.[34] As shown in Figure 2a, the NMR spectrum of calcined H-BEA-18 contains an additional resonance at ∼0 ppm. This shift is indicative of octahedral Al, which can act as a Lewis acid, either within the framework at lattice defect sites[38] or as extra-framework Al. The octahedral Al is largely stable to reaction conditions, as shown in Figure 2a and Table S1. To determine whether the octahedral Al is the active site for fructose−glucose isomerization, we washed H-BEA-18 with HCl at pH = 1 for 16 h according to the procedure of Hey et al.[39] This procedure results in substantial reduction of the 0 ppm peak, as shown in Figure 2a. The ratios of octahedral-to-tetrahedral Al of the different samples were calculated by integrating the corresponding NMR peaks, and are shown in Table S1. Figure 2b shows that removal of the octahedral Al significantly reduces glucose selectivity and significantly increases levulinic acid selectivity. Thus, the octahedral Al is indeed responsible for the isomerization activity, and likely some side reactions of HMF or levulinic acid.

Furthermore, ^{13}C and ^{1}H NMR investigation of fructose produced from deuterium-labeled glucose-D-2 (deuterated at C2 position) isomerization (Figure 3), following the analysis of Román-Leshkov et al.,[40] shows that H-BEA-18 catalyzes the isomerization reaction via an intramolecular hydride shift mechanism analogous to the Lewis acid Sn-BEA zeolite.[40] The deuterium at the C2 position of the glucose-D-2 is transferred to the C1 position of the product fructose in the intramolecular hydride shift pathway, whereas no deuterium is observed in the product fructose for the proton transfer mechanism. Briefly, the glucose spectra remained unchanged after the reaction, suggesting that there is no deuterium−hydrogen exchange with the solvent during the course of the reaction. The resonances at δ = 63.8 and 62.6 ppm assigned to the C1 position of the β-fructopyranose and β-fructofuranose of the unlabeled fructose in the ^{13}C spectrum appeared as low intensity triplets. This reduction in the peak intensity is explained by the absence of a nuclear Overhauser enhancement effect due to the presence of a deuterium atom at C1 of the product fructose. This is further confirmed by ^{1}H NMR analysis. Significant differences between the ^{1}H NMR spectra of the product fructose and unlabeled fructose (control) were observed. Particularly, the resonance at 3.45 ppm in the ^{1}H spectrum of fructose produced by H-BEA-18 catalyzed isomerization was absent due to the presence of a deuterium

dx.doi.org/10.1021/cs4002157 | ACS Catal. 2013, 3, 1279−1291

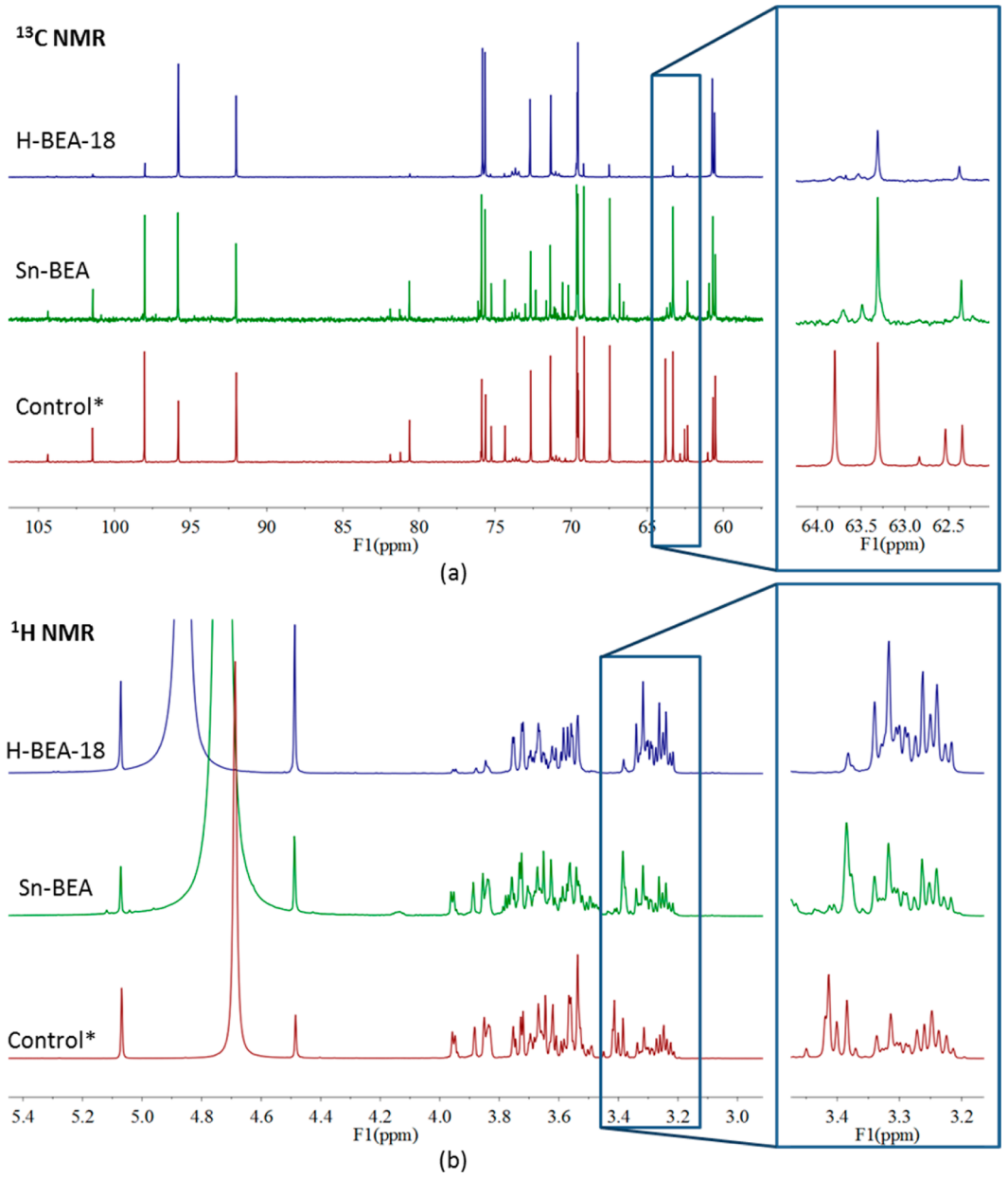

Figure 3. (a) ^{13}C and (b) ^{1}H NMR of the sugar fraction from glucose-D-2 isomerization with H-BEA-18 and Sn-BEA zeolites. Control*: physical mixture of glucose-D-2 and unlabeled fructose in water.

atom at C1 of the product fructose. Overall, these findings from ^{13}C and ^{1}H NMR analysis confirm an intramolecular hydride transfer pathway as the dominant reaction channel for glucose-to-fructose isomerization using H-BEA-18 analogous to the Sn-BEA catalyzed isomerization.

The selectivity to glucose in Figure 1 appears to plateau, which is likely due to the relative kinetics of isomerization and reactions to other (known and unknown) products. The equilibrium constant at 130 °C for the isomerization of fructose to glucose[41] is on the order of K_{eq} = [Glu]/[Fru] = 0.59, which is at least a factor of 5 larger than the [Glu]/[Fru] ratio observed in the reaction solutions. Furthermore, [Glu]/[Fru] increases monotonically through 5 h of reaction time, as shown in Figure S2, suggesting that the isomerization reaction is not equilibrated.

For completeness, we also examined whether H-BEA-18 catalyzes the isomerization of glucose to fructose. When glucose was used as a reagent, the conversion at 5.5 h is ∼10%, and fructose is generated in approximately 50% selectivity (Figure S3). This further corroborates the fact that the octahedral Al (Lewis acid site) leads to aldose−ketose isomerization. As with the fructose reagent, the concentrations of glucose and fructose with a glucose reagent are far from the calculated equilibrium at 130 °C (Figure S2).

The increase in fructose conversion with H-BEA-18 compared to the homogeneous reaction does not result solely from the isomerization of fructose to glucose. Depending on the catalyst loading and reaction time, the change in moles of fructose converted relative to the homogeneous case is between two and six times larger than the moles of glucose formed. The difference can be seen explicitly in Figure 4, which shows the initial rates of fructose consumption and production of glucose, HMF, and levulinic acid as a function of aluminum-to-fructose molar ratio (Al/Fru). Total fructose consumption increases

dx.doi.org/10.1021/cs4002157 | ACS Catal. 2013, 3, 1279−1291

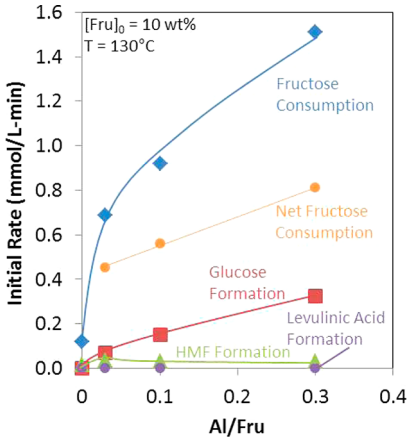

Figure 4. Initial rates of fructose consumption, glucose production, HMF production, and levulinic acid production. Lines are shown only to guide the eye. The homogeneous case corresponds to points on the *y* axis (Al/Fru = 0). Net fructose consumption refers to the rate of fructose consumption after subtracting fructose adsorption, the homogeneous fructose consumption rate, and the formation rate of glucose, HMF, and levulinic acid. Net fructose consumption is related to the rate of zeolite-catalyzed humin formation.

with catalyst loading, due to adsorption on the catalyst, and isomerization, dehydration, and other reactions. While fructose adsorption and glucose isomerization both increase linearly with catalyst loading (the former because the initial concentration of fructose is in the Henry's Law regime[42]), the initial net rate of fructose consumption (after subtracting homogeneous, isomerization, and dehydration rates and fructose adsorption) also increases with zeolite loading. Additionally, the rate of the dehydration pathway (the sum of the HMF and levulinic acid formation rates) is essentially constant with zeolite loading. These trends confirm that the zeolite catalyzes side reactions of fructose.

Figure 4 also shows that homogeneous chemistry, indicated by the left-most fructose consumption point, contributes a significant fraction to the overall chemistry, especially at low catalyst loadings. On the basis of these initial rates, around 15% of initial fructose consumption at Al/Fru = 0.03 can be attributed to homogeneous chemistry. This result implies that efforts to model fructose dehydration reactors must include both homogeneous and heterogeneous reaction mechanisms, especially at low catalyst loadings.

3.2. Mechanisms of Zeolite Contribution to Dehydration Chemistry of Sugars. The above experiments indicate that H-BEA-18 is active for side reactions of fructose and the desired products HMF, levulinic acid, and furfural. We hypothesized four mechanisms by which the zeolite may catalyze these side reactions, as shown in Scheme 2. These mechanisms include preferential adsorption of the desired products that leads to further reaction, catalysis by dissolved framework species, homogeneous Brønsted acid catalysis resulting from dissociation of Brønsted sites and surface silanols, and reactions at the zeolite particle external surface.

3.2.1. Preferential Adsorption and Reaction of Desired Products. Two distinct effects can arise from preferential adsorption of desired products. First, if desired products remain adsorbed to the catalyst surface, apparent selectivity measured from aqueous-phase product concentrations will be lower than the actual selectivity. Because adsorption capacities of many solid catalysts for the components in fructose dehydration reaction mixtures have not been measured, it is unknown how large of a role adsorption generally plays in determining selectivity. Second, if desired products are strongly adsorbed at reaction temperatures, further reaction can occur. Thus, conversion and selectivity of the desired products must also be explored to understand the effects of catalyst adsorption on product distribution.

To determine experimentally the potential contribution of preferential adsorption to the observed selectivity trends, used zeolite (Al/Fru = 0.30) was filtered and resuspended in a known volume of water, equilibrated for 24 h at room temperature, and filtered a second time. HPLC analysis of the resuspended solution then gives an estimate of the fraction of each analyte adsorbed on the catalyst. The experimental procedure is shown in Scheme 4.

The absolute amount of each species adsorbed is similar for all products, as shown in Figure 5. Thus, the selectivity trends reported above should not be significantly altered by adsorption. However, the relative amount of each species varies considerably. The yields of fructose and glucose desorbed after one resuspension cycle were on the order of 13% of the total yield (reaction plus resuspended). Around 16% of the formic acid was adsorbed. However, the yields of levulinic acid, HMF, and furfural in the resuspended solution were 23%, 28%, and 41%, respectively, of the total yields. These values follow the same trend observed for single component isotherms of each species[42] and are qualitatively consistent with experiments of Weingarten et al.,[43] who also observed a much higher uptake of furfural on an H-FAU-Y zeolite than on the other solid acid catalysts used in their xylose dehydration experiments. The values reported here should be considered upper limits because the highest zeolite loading was used for the resuspension experiments and a small amount of the original reaction liquid was necessarily resuspended with the zeolite due to capillary forces between particles. Overall, adsorption of furanic compounds and levulinic acid and to a lesser extent of sugars needs to be accounted for in understanding product

Scheme 4. Flow Chart for Measuring Fraction of Adsorbed Compounds

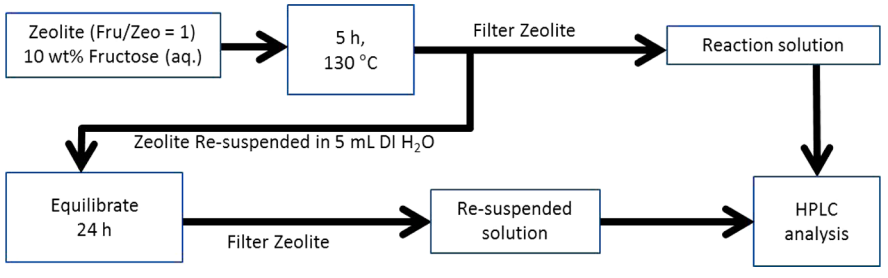

dx.doi.org/10.1021/cs4002157 | ACS Catal. 2013, 3, 1279–1291

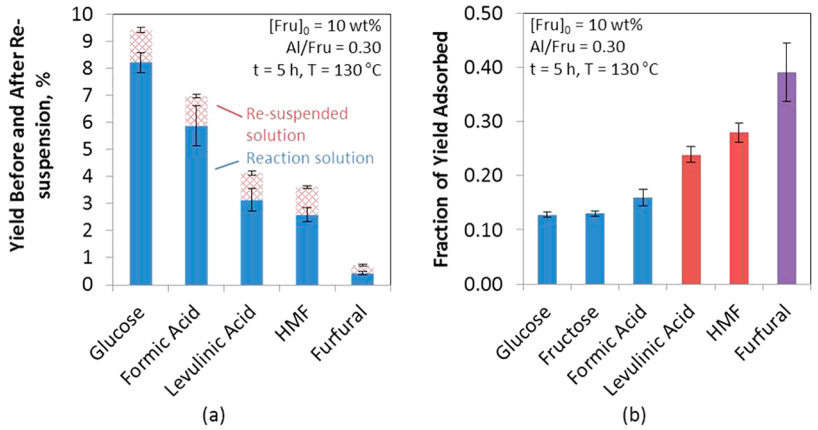

Figure 5. (a) Yields of each product before and after one resuspension cycle. (b) Fraction of each analyte detected in resuspended solution relative to total cumulative yield. Error bars represent the standard deviation of three replicates.

distribution and yields in the heterogeneous conversion of sugars to furans.

It is important to note that this strong adsorption can lead to further reaction of the desired products, which we explored by reacting solutions of levulinic acid, furfural, and HMF with and without H-BEA-18 catalyst. Each of the compounds is relatively stable in aqueous solution at 130 °C, giving negligible conversion of levulinic acid and furfural, and around 10% conversion for HMF. However, H-BEA-18 significantly increases consumption, as shown in Figure 6. Total

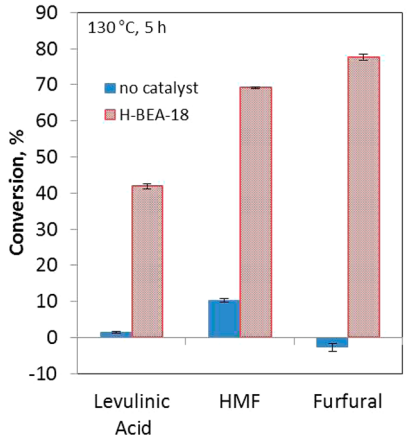

Figure 6. Consumption of levulinic acid, HMF, and furfural in the presence and absence of H-BEA-18 zeolite. For H-BEA-18 data, zeolite loading was equivalent to Al/Fru = 0.10 for the 10 wt % fructose data. Initial concentrations were 0.1 wt %, 0.25 wt %, and 0.027 wt % for levulinic acid, HMF, and furfural, respectively. These concentrations were selected to match concentrations observed in experiments starting with 10 wt % fructose. Error bars represent the standard deviation of at least two replicates.

consumption of levulinic acid, HMF, and furfural with H-BEA-18 is 42%, 69%, and 78%, respectively. The increase is likely due to both adsorption and reaction, as the consumption is a factor of 1.8−2.5 larger than the upper limit attributable to adsorption (from Figure 5).

We further investigated zeolite activity with HMF as a reagent, as shown in Figure 7. A solution of 0.25 wt % HMF (approximately the highest concentration observed with fructose as reagent) was reacted in water with H-BEA-18, without H-BEA-18 at an initial pH of 4.9 (unmodified pH), and

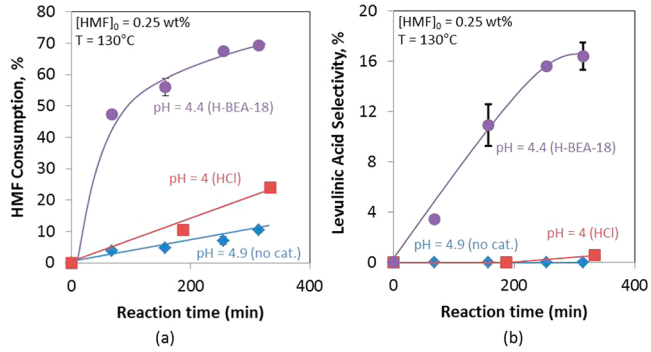

Figure 7. Conversion (a) and selectivity (b) of rehydration chemistry of 0.25 wt % HMF with and without H-BEA-18. The pH values shown are initial pH values. pH decreased during the reaction; see runs 16−18 in Table 1 for final pH values. Error bars represent the standard deviation of at least two replicates.

an initial pH of 4 (acidified with HCl to account for homogeneous Brønsted acidity introduced by the zeolite, as discussed below). Without H-BEA-18 or HCl, conversion is ≤10%, and unknown products (i.e., neither formic nor levulinic acid) account for nearly all of the reacted HMF. Acidifying the water to pH = 4 increases the conversion to 25%, but selectivity to levulinic acid remains below 2%. In comparison to the sugars discussed below, the initial drop of the pH by the addition of zeolite may have a modest accelerating effect on the conversion of HMF.

With the H-BEA-18 catalyst, however, conversion at 5 h increases to 70%, and selectivity to levulinic acid increases to 15%. That is, the zeolite increases HMF conversion and levulinic acid selectivity by a factor of at least 2.9 and 29.0, respectively, compared to the homogeneous case.

The enhanced selectivity to rehydration products does not account for all of the increased conversion, indicating that H-BEA-18 also reduces the HMF concentration by other means, such as polymerization or adsorption. Some evidence of polymerization was observed in the HPLC chromatogram, as a peak with an area of 2−3 times the levulinic acid peak was observed at a retention time between 7 and 8 min. This retention time is similar to the fructose dimer, difructose anhydride. Thus, this peak might represent an HMF dimer, but the exact identity and structure could not be unequivocally determined. The peak area was roughly 2 orders of magnitude

dx.doi.org/10.1021/cs4002157 | ACS Catal. 2013, 3, 1279−1291

smaller in the absence of H-BEA-18. Thus, H-BEA-18 likely catalyzes HMF polymerization in addition to rehydration.

Interestingly, in comparison to the work of Ordomsky et al. with an H-BEA catalyst,[32] the initial HMF consumption rate is similar (~50% conversion after 90 min reaction time), despite the higher HMF concentration and temperature used in that work. Ordomsky et al. also noted only the production of oligomerization products but not of formic and levulinic acids. The reasons for the discrepancy are not clear at this point but may be due to the favored formation of the acids at lower temperatures.[44]

The negative effects of preferential adsorption can be partially mitigated by the use of an organic extracting phase, such as methyl isobutyl ketone (MIBK). Figure 8 shows that

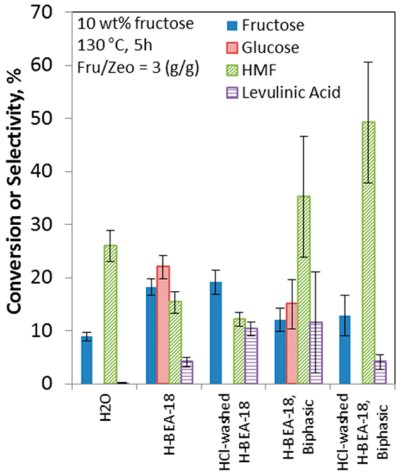

Figure 8. Effect of MIBK as organic extracting phase at 130 °C and 5 h reaction time. Furfural could not be resolved from MIBK in the HPLC analysis. Conversion and selectivity reflect cumulative compound concentrations from both the aqueous and organic phases. Error bars represent the standard deviation of at least two replicates.

selectivity to HMF and levulinic acid can be significantly increased by the addition of MIBK, which selectively partitions the desired products away from zeolite active sites and the aqueous phase, inhibiting further reaction to undesirable side products. The selectivity can be further improved if a zeolite without extra-framework Al is used, as shown in the rightmost set of bars in Figure 8. The reduction of side reactions leads to a decrease in fructose conversion.

It is important to note that adsorption and side reactions can affect apparent carbon balances based on HPLC analysis. Carbon errors were typically <10% but increased as reaction time and catalyst loading increased. As a limiting case, with Al/Fru = 0.30 at a 5 h reaction time, the carbon balance was ~18% short. Approximately 13% could be attributed to adsorption of fructose and known products, leaving a 5% error due to other causes. This adsorption value was obtained by recalculating concentrations of glucose, fructose, formic acid, levulinic acid, HMF, and furfural using HPLC peak areas of each component that were increased by the yield ratio, R, for the resuspended and reaction solutions (e.g., $R_{furfural} = Y_{resuspended}/Y_{reaction} = 0.28\%/0.44\% = 0.64$). The remainder of missing carbon is likely due primarily to the formation of fragmentation products that were observed in small amounts but not quantified (lactic acid, pyruvic acid, pyruvaldehyde, dihydroxyacetone, and glyceraldehyde) and polymers of fructose and HMF. The polymers are formed by condensation and dehydration reactions that produce initially unknown products with HPLC retention times indicative of soluble oligomers, and eventually deeply colored species not detected by HPLC.[45] The distribution of unknown products with HPLC-RID retention times indicative of soluble oligomeric products was slightly different in the presence of H-BEA-18 than in the homogeneous case (Figure S4), consistent with the hypothesis that the zeolite catalyzes side reactions.

3.2.2. Dissolution by Acidic Products. Because zeolite dissolution via dealumination in water is enhanced by acids,[46] acidic products formed in the reaction may lead to a loss of aluminum from the framework. Potential dissolution of the zeolite was initially explored by heating the zeolite suspension in water at pH ~5.6, and in formic acid and HCl at pH = 3. The zeolite was filtered from these solutions, and the filtrate was used as a solvent for the homogeneous dehydration of 10 wt % fructose. Comparison of this "Zeolite Filtrate (ZF)" experiment to homogeneous dehydration (both unmodified and initial pH = 3 with formic acid and HCl) and H-BEA-18 heterogeneous experiments is shown in Figure 9. It appears that homogeneous

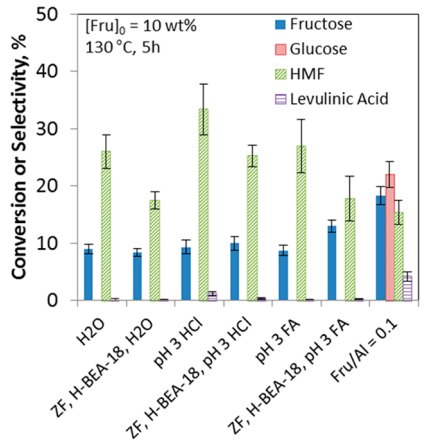

Figure 9. Fructose conversion and selectivity to glucose, HMF, and levulinic acid from 10 wt % aqueous fructose at 130 °C in homogeneous solution (unmodified pH in water and controlled pH using HCl or formic acid (FA)), zeolite filtrate (ZF), and solid H-BEA-18 dehydration experiments.

chemistry induced by species dissolved from the zeolite decreases considerably HMF selectivity. ICP analysis of the zeolite filtrate and reaction solutions confirmed the presence of aluminum and silicon species, as shown in Figure 9 and Table 2. These concentrations correspond to 0.8−4.4 mM Al and 4.9−8.0 mM Si.

Upon increasing the zeolite loading (entries 4−6 in Table 2), the Al concentration increases roughly proportionally, while the Si concentration does not increase significantly. Thus, dissolution of the Si framework may be limited by solubility at pH ~3, while dealumination is not. The observed Si concentrations are slightly higher than those reported in the literature for SiO_2 solubility equilibrium,[47−49] corresponding to the higher temperatures in the current experiments.[50] The chemistry of the dissolved species is complex, and thus, a detailed description is outside the scope of the current experiments. We will report a more in-depth characterization of these dissolved species in a follow-up manuscript.[51]

Although the zeolite is partially dissolved during reaction, the performance of the residual catalyst is not significantly affected

dx.doi.org/10.1021/cs4002157 | ACS Catal. 2013, 3, 1279−1291

Table 2. Concentrations of Al and Si in H-BEA-18 Zeolite Filtrate (ZF) and Reaction Solutions Determined by ICP

entry	solution	Al (mg/L)	% of total Al dissolved	Si (mg/L)	% of total Si dissolved
1	ZF, H_2O	0.0	0.0	105.9	0.8
2	ZF, HCl	2.8	0.2	120.0	0.9
3	ZF, formic acid	16.0	1.1	137.8	0.9
4	Al/Fru = 0.00, 5 h	1.2		7.4	
5	Al/Fru = 0.10, 5 h	42.5	2.8	201.8	1.4
6	Al/Fru = 0.30, 5 h	118.9	2.6	223.7	0.5

through three reuse cycles, as shown in Figure 10. Calcination between reuse cycles moderately enhances isomerization

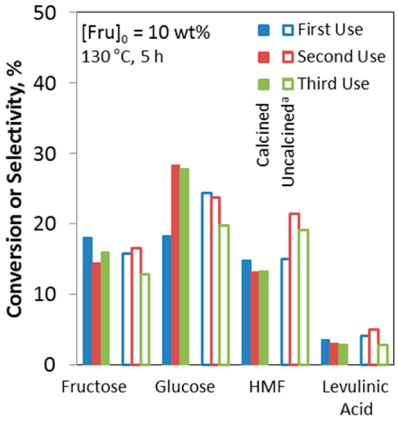

Figure 10. Performance of H-BEA-18 through three cycles. Calcined before first use.

activity, likely due to increased extra-framework Al generated by the calcination, as discussed above. Similarly, the BET total and external surface area, micropore volume, median pore width, and acid site density can be regenerated by calcination after reaction, as shown in Table 3, suggesting that the structure

Table 3. Characterization of H-BEA-18 before and after Reaction[a]

catalyst	BET surface area (m^2/g)	external surface area (m^2/g)	t-plot micropore volume (cm^3/g)	SiO_2/Al_2O_3	acid site density (mmol H^+/g)
H-BEA-18	641.3	237.5	0.165	18.7	0.88
H-BEA-18 postreaction, calcined	646.1	244.6	0.164	17.8	0.84

[a]Surface area, pore volume, and median pore width determined by N_2 physisorption, SiO_2/Al_2O_3 ratio by ICP analysis of digested zeolite, and acid site density by TGA of adsorbed isopropylamine.

of the catalyst is not significantly affected. Similarly, the SiO_2/Al_2O_3 ratio remained constant within experimental error before and after reaction (Table 3). These analyses are consistent with TGA analysis, which showed the amount of the deposits to be insignificant, and with the small fraction of Al dissolved during reaction.

3.2.3. Zeolite-Induced Change of Solution pH. The solution pH decreases upon adding zeolite and throughout the reaction. This decrease is likely due to proton delocalization from Brønsted sites and surface silanol groups (Scheme 2). Additionally, the pH decreased less through the course of reaction with zeolite than in the homogeneous case, and when zeolite was added to pH 3 formic acid or HCl, the solution pH increased. This effect has been studied in depth for a variety of oxide materials by Regalbuto et al.,[52,53] and for silicalite-1 by Nikolakis et al.[54] These observations can be partially explained by a tendency of the zeolite surface to buffer the solution pH toward the pH at which the zeolite surface has zero net charge, or the point of zero charge (pH_{PZC}), by protonation and deprotonation of surface hydroxyl groups. H-BEA-18 exhibits a $pH_{PZC} \sim 4.0$ based on an approximation of the mass titration method,[55] as shown in Figure S6. However, we note that upon filtering the aqueous zeolite suspensions, zeolite filtrates of higher pH than pH_{PZC} returned to their original pH while those with pH below pH_{PZC} did not. Thus, adsorption and reaction of acidic products likely play a role in the observed buffering effect; acid adsorption is also a feature predicted by Regalbuto et al.[53,56−59]

To investigate whether the change in initial pH contributes significantly to the observed chemistry, 10 wt % fructose was dehydrated in water with initial pH = 4 (acidified with HCl) without zeolite. This pH value was chosen for comparison to the lowest initial pH observed with H-BEA-18, as shown in Table 1. Figure 11 shows that the change of the initial pH has

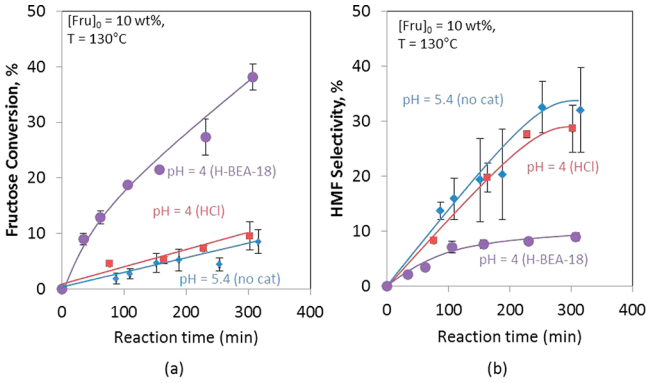

Figure 11. Effect of pH and zeolite on fructose conversion (a) and HMF selectivity (b). For pH = 4 (H-BEA-18), Al/Fru = 0.30. Error bars represent the standard deviation of at least two replicates.

only a minor effect (within statistical error) on fructose conversion and HMF selectivity. Selectivities to other quantified products were also similar to the nonacidified homogeneous reaction. The addition of zeolite leads to much higher conversion of fructose, consistent with the findings discussed above that, for higher zeolite loadings, the main chemistry is heterogeneous.

In summary, the change in chemistry induced by the zeolite is not primarily due to the lower initial solution pH as one may expect. Instead, the generation of acidic products early in the reaction quickly becomes the controlling factor of the solution pH.

3.2.4. Reactions at Zeolite External Surface. To explore whether surface Al atoms affect the observed chemistry, H-BEA-18 was passivated with a solution of TEOS, which covers the surface of the zeolite with a layer of amorphous SiO_2. XRD analysis showed that the TEOS-passivated sample had ~90% crystallinity relative to the unpassivated H-BEA-18,[60,61] which is

dx.doi.org/10.1021/cs4002157 | ACS Catal. 2013, 3, 1279−1291

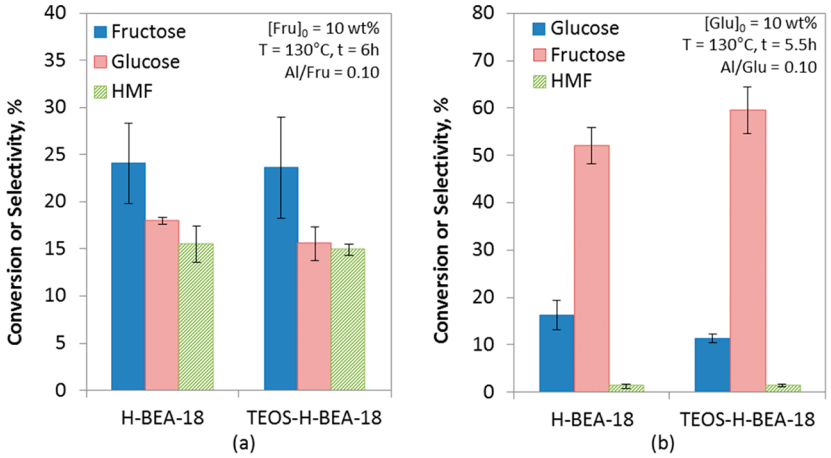

Figure 12. (a) Effect of TEOS surface passivation of zeolite on fructose conversion, HMF selectivity, and glucose selectivity. (b) Effect of TEOS surface passivation of zeolite on glucose conversion, HMF selectivity, and fructose selectivity. Error bars represent the standard deviation of at least two replicates.

close to the range observed by other researchers for a similar treatment.[32] No precipitate was formed after 48 h from a mixture of 5 vol % TEOS in hexane, which precludes the possibility that changes in the passivated catalyst could be from "dilution" of the zeolite by amorphous SiO_2 particles precipitated during the passivation procedure. The comparison between fructose conversion and selectivity to HMF and glucose using TEOS-passivated and unpassivated H-BEA-18 are shown in Figure 12a. It can be seen that surface passivation has very little effect on the observed dehydration chemistry. Ordomsky et al.[32] also noted that surface passivation of H-BEA has only a minor effect, likely due to the low strength of the acid sites. However, the selectivity to glucose is slightly lower with TEOS-H-BEA-18 than with H-BEA-18, suggesting that the surface sites might not be entirely irrelevant in isomerization. With glucose as a reagent, the glucose conversion is lower with TEOS-H-BEA-18 than with H-BEA-18, but the selectivity to fructose is slightly higher (Figure 12b). The difference for glucose and fructose may be explained from the different reactivities of the two isomers. That is, with the less reactive glucose, isomerization represents a larger fraction of the total chemistry, and there is almost no homogeneous reaction (Figure S3). Thus, the effect of surface passivation is more apparent, resulting in a lower conversion and higher isomerization selectivity. In general, however, the role of surface acid sites appears to be minor.

3.4. Broader Impacts. There are several implications for aqueous sugar processing to furan and acid derivatives with zeolite catalysts that are clarified from these experiments. First, the desired HMF product must be separated from the zeolite and water in order to be obtained in appreciable yields. This has been known for many years[62,63] but is difficult to achieve in many zeolites because of the relatively strong adsorption of HMF on the catalyst that leads to its further reaction. Second, the zeolite is active for HMF rehydration to levulinic acid and formic acid. These acidic products react with the zeolite to produce species that decrease selectivity to the fructose dehydration pathway. Although the production of levulinic acid from aqueous HMF with zeolite catalysts may have limited utility under these conditions, it may be commercially viable if the acids can be selectively removed from the reaction medium. Additionally, these experiments indicate that at high catalyst loadings, heterogeneous chemistry dominates over homogeneous, and thus, designing catalysts to improve yields of either HMF or levulinic acid from aqueous sugars may be feasible.

Conversely, we have also shown that both homogeneous and heterogeneous reactions can take place in parallel and that both need to be considered for meaningful analysis. The exact contribution of each chemistry to the overall rate is expected to be condition-dependent. For example, as the ratio of catalyst to liquid volume increases, the contribution of homogeneous chemistry would decrease, as expected in all homogeneous/heterogeneous reactions. The relative amounts of aqueous solution and catalyst provide a simple and rational approach to controlling the contribution of each chemistry. One complication in quantitatively controlling this contribution arises from dissolution of aluminum and silicon species from the zeolite that contribute to the homogeneous chemistry, i.e., zeolite-induced homogeneous chemistry. This creates naturally a coupling between chemistries.

4. CONCLUSIONS

We have conducted a set of experiments to elucidate the main routes by which a zeolite can affect dehydration of sugars (fructose and glucose) to HMF and HMF rehydration to levulinic acid in aqueous solutions. We have used an acidic BEA zeolite (H-BEA-18) as a representative acid catalyst, but other zeolites show similar trends. Specifically, we have delineated the relative role of homogeneous chemistry (both solvent- and zeolite-induced), the effect of external surface acid sites, and the effect of adsorption of products and reactants on the catalyst for these reactions.

We have found that H-BEA-18 increases the conversion of fructose and HMF in part by catalyzing fructose isomerization to glucose and HMF rehydration to formic and levulinic acids, respectively. The glucose-to-fructose isomerization and its reverse are caused by octahedral aluminum atoms that act as Lewis acid sites either within the framework at lattice defect sites or as extra-framework Al. These sites are formed during calcination, are stable under reaction conditions, and are also able to catalyze some reactions to unknown products from both fructose and HMF.

The acids produced from HMF rehydration dissolve aluminosilicate species from the zeolite, which also catalyze some of the undesired side reactions. While the addition of zeolites to an aqueous solution decreases the initial pH

dx.doi.org/10.1021/cs4002157 | ACS Catal. 2013, 3, 1279−1291

considerably, this change contributes negligibly to the homogeneous chemistry. This is probably due to the formation of acids (e.g., from the rehydration of HMF) that reduce and control the pH during reaction soon after reaction starts. External surface passivation experiments indicate that reactions catalyzed by external surface Al atoms do not significantly alter the observed chemistry under our conditions.

H-BEA-18 more readily converts HMF than fructose, an observation that is reflected in relative adsorption uptakes, which show strong preferential adsorption of HMF, furfural, and levulinic acid. As a result, the HMF produced by fructose dehydration is converted into levulinic and formic acids (along with other undesired products). Under mildly acidic conditions (without addition of inorganic acids) that are environmentally preferred, zeolites can increase the conversion of HMF and the selectivity to levulinic acid many-fold. In conjunction with using a biphasic system, the selectivity to HMF and levulinic acid can be increased. This provides an indication that heterogeneous materials may be superior in the production of levulinic acid from HMF.

■ ASSOCIATED CONTENT

Supporting Information

Supporting Information is available with full kinetic data, tetrahedral-to-octahedral Al ratios of H-BEA-18 through calcination and reaction treatments, glucose/fructose equilibrium constants, glucose reaction data, sample chromatograms, X-ray diffractograms, and mass titration data for H-BEA-18 zeolite. This material is available free of charge via the Internet at http://pubs.acs.org

■ AUTHOR INFORMATION

Corresponding Author

*E-mail: vlad@udel.edu (V.N.), vlachos@udel.edu (D.G.V.).

Notes

The authors declare no competing financial interest.

■ ACKNOWLEDGMENTS

The work was financially supported from the Catalysis Center for Energy Innovation, an Energy Frontier Research Center funded by the U.S. Department of Energy, Office of Science, Office of Basic Energy Sciences under Award Number DE-SC0001004. The authors would also like to thank Dr. Shuyu Hou and Prof. Kelvin Lee for assistance with HPLC-MS/MS data acquisition and analysis, Drs. Guangjin Hou and Steve Bai for assistance with ^{27}Al NMR spectroscopy, Ana B. Pinar for Sn-BEA synthesis, Ms. Cathy Olsen for assistance with ICP analysis, and Chun-Chih Chang and Prof. Wei Fan at the University of Massachusetts—Amherst for quantification of acid sites.

■ REFERENCES

(1) Werpy, T.; Petersen, G. *Top Value Added Chemicals from Biomass: Vol. I - Results of Screening for Potential Candidates from Sugars and Synthesis Gas*; National Renewable Energy Lab: Golden, CO, 2004.
(2) Lewkowski, J. *ARKIVOC* **2001**, *2001*, 17−54.
(3) Karinen, R.; Vilonen, K.; Niemelä, M. *ChemSusChem* **2011**, *4*, 1002−1016.
(4) Moreau, C.; Belgacem, M. N.; Gandini, A. *Top. Catal.* **2004**, *27*, 11−30.
(5) Rauter, A. P.; Xavier, N. M.; Lucas, S. D.; Santos, M.: Chapter 3 - Zeolites and Other Silicon-Based Promoters in Carbohydrate Chemistry. In *Adv. Carbohydr. Chem. Biochem.*; Horton, D., Ed.; Academic Press: New York, 2010; Vol. *63*; pp 29−99.
(6) Tong, X.; Ma, Y.; Li, Y. *Appl. Catal., A* **2010**, *385*, 1−13.
(7) Vigier, K.; Jérôme, F.: Heterogeneously-Catalyzed Conversion of Carbohydrates. In *Carbohydrates in Sustainable Development II*; Rauter, A. P., Vogel, P., Queneau, Y., Eds.; Springer: Berlin/Heidelberg, 2010; Vol. *295*; pp 63−92.
(8) Perego, C.; Bosetti, A. *Microporous Mesoporous Mater.* **2011**, *144*, 28−39.
(9) Taarning, E.; Osmundsen, C. M.; Yang, X.; Voss, B.; Andersen, S. I.; Christensen, C. H. *Energy Environ. Sci.* **2011**, *4*, 793−804.
(10) Moreau, C.; Durand, R.; Razigade, S.; Duhamet, J.; Faugeras, P.; Rivalier, P.; Ros, P.; Avignon, G. *Appl. Catal., A* **1996**, *145*, 211−224.
(11) Jow, J.; Rorrer, G. L.; Hawley, M. C.; Lamport, D. T. A. *Biomass* **1987**, *14*, 185−194.
(12) Lourvanij, K.; Rorrer, G. L. *Ind. Eng. Chem. Res.* **1993**, *32*, 11−19.
(13) Moreau, C.; Durand, R.; Pourcheron, C.; Razigade, S. *Ind. Crops Prod.* **1994**, *3*, 85−90.
(14) Lourvanij, K.; Rorrer, G. L. *J. Chem. Technol. Biotechnol.* **1997**, *69*, 35−44.
(15) Lourvanij, K.; Rorrer, G. L. *Appl. Catal., A* **1994**, *109*, 147−165.
(16) Shi, Y.; Li, X.; Hu, J.; Lu, J.; Ma, Y.; Zhang, Y.; Tang, Y. *J. Mater. Chem.* **2011**, *21*, 16223−16230.
(17) Takagaki, A.; Ohara, M.; Nishimura, S.; Ebitani, K. *Chem. Commun.* **2009**, 6276−6278.
(18) Agirrezabal-Telleria, I.; Requies, J.; Güemez, M. B.; Arias, P. L. *Appl. Catal., B* **2012**, *115−116*, 169−178.
(19) Dias, A. S.; Lima, S.; Pillinger, M.; Valente, A. A. *Carbohydr. Res.* **2006**, *341*, 2946−2953.
(20) Dias, A.; Lima, S.; Brandão, P.; Pillinger, M.; Rocha, J.; Valente, A. *Catal. Lett.* **2006**, *108*, 179−186.
(21) Dias, A. S.; Pillinger, M.; Valente, A. A. *Microporous Mesoporous Mater.* **2006**, *94*, 214−225.
(22) Dias, A.; Lima, S.; Pillinger, M.; Valente, A. *Catal. Lett.* **2007**, *114*, 151−160.
(23) Kim, S.; You, S.; Kim, Y.; Lee, S.; Lee, H.; Park, K.; Park, E. *Korean J. Chem. Eng.* **2011**, *28*, 710−716.
(24) Lima, S.; Pillinger, M.; Valente, A. A. *Catal. Commun.* **2008**, *9*, 2144−2148.
(25) Lima, S.; Antunes, M. M.; Fernandes, A.; Pillinger, M.; Ribeiro, M. F.; Valente, A. A. *Appl. Catal., A* **2010**, *388*, 141−148.
(26) Lima, S.; Fernandes, A.; Antunes, M.; Pillinger, M.; Ribeiro, F.; Valente, A. *Catal. Lett.* **2010**, *135*, 41−47.
(27) Lima, S.; Antunes, M. M.; Fernandes, A.; Pillinger, M.; Ribeiro, M. F.; Valente, A. A. *Molecules* **2010**, *15*, 3863−3877.
(28) Shi, X.; Wu, Y.; Li, P.; Yi, H.; Yang, M.; Wang, G. *Carbohydr. Res.* **2011**, *346*, 480−487.
(29) Zhang, J.; Zhuang, J.; Lin, L.; Liu, S.; Zhang, Z. *Biomass Bioenerg.* **2012**, *39*, 73−77.
(30) Kruger, J. S.; Nikolakis, V.; Vlachos, D. G. *Curr. Opin. Chem. Eng.* **2012**, *1*, 312−320.
(31) Weber, R. W.; Möller, K. P.; O'Connor, C. T. *Microporous Mesoporous Mater.* **2000**, *35−36*, 533−543.
(32) Ordomsky, V. V.; Schaaf, J. v. d.; Schouten, J. C.; Nijhuis, T. A. *J. Catal.* **2012**, *287*, 68−75.
(33) Valencia, S. V.; Canos, A. C.: Stannosilicate molecular sieves. U.S. Patent No. 5,968,473, 1999.
(34) Shetti, V. N.; Kim, J.; Srivastava, R.; Choi, M.; Ryoo, R. *J. Catal.* **2008**, *254*, 296−303.
(35) Williams, C. L.; Chang, C.-C.; Do, P.; Nikbin, N.; Caratzoulas, S.; Vlachos, D. G.; Lobo, R. F.; Fan, W.; Dauenhauer, P. J. *ACS Catal.* **2012**, *2*, 935−939.
(36) Biaglow, A. I.; Parrillo, D. J.; Gorte, R. J. *J. Catal.* **1993**, *144*, 193−201.
(37) Beers, A. E. W.; van Bokhoven, J. A.; de Lathouder, K. M.; Kapteijn, F.; Moulijn, J. A. *J. Catal.* **2003**, *218*, 239−248.

(38) Kunkeler, P. J.; Zuurdeeg, B. J.; van der Waal, J. C.; van Bokhoven, J. A.; Koningsberger, D. C.; van Bekkum, H. *J. Catal.* **1998**, *180*, 234−244.
(39) Hey, M. J.; Nock, A.; Rudham, R.; Appleyard, I. P.; Haines, G. A. J.; Harris, R. K. *J. Chem. Soc., Faraday Trans. 1* **1986**, *82*, 2817−2824.
(40) Román-Leshkov, Y.; Moliner, M.; Labinger, J. A.; Davis, M. E. *Angew. Chem., Int. Ed.* **2010**, *49*, 8954−8957.
(41) Moliner, M.; Román-Leshkov, Y.; Davis, M. E. *Proc. Natl. Acad. Sci. U. S. A.* **2010**, *107*, 6164−6168.
(42) Leon-Garcia, M.; Nikolakis, V.; Vlachos, D. G. *Langmuir* In press. 10.1021/la401138g.
(43) Weingarten, R.; Tompsett, G. A.; Conner, J. W. C.; Huber, G. W. *J. Catal.* **2011**, *279*, 174−182.
(44) Weingarten, R.; Cho, J.; Xing, R.; Conner, W. C.; Huber, G. W. *ChemSusChem* **2012**, *5*, 1280−1290.
(45) Suárez-Pereira, E.; Rubio, E. M.; Pilard, S.; Ortiz Mellet, C.; García Fernández, J. M. *J. Agric. Food Chem.* **2009**, *58*, 1777−1787.
(46) Yang, C.; Xuaf, Q. *Zeolites* **1997**, *19*, 404−410.
(47) Iler, R. K. *J. Colloid Interface Sci.* **1973**, *43*, 399−408.
(48) Krauskopf, K. B. *Geochim. Cosmochim. Acta* **1956**, *10*, 1−26.
(49) Jander, G.; Heukeshoven, W. *Z. Anorg. Allg. Chem.* **1931**, *201*, 361−382.
(50) Alexander, G. B.; Heston, W. M.; Iler, R. K. *J. Phys. Chem.* **1954**, *58*, 453−455.
(51) Kruger, J. S.; Nikolakis, V.; Vlachos, D. G. In Preparation.
(52) Park, J.; Regalbuto, J. R. *J. Colloid Interface Sci.* **1995**, *175*, 239−252.
(53) Agashe, K. B.; Regalbuto, J. R. *J. Colloid Interface Sci.* **1997**, *185*, 174−189.
(54) Nikolakis, V.; Tsapatsis, M.; Vlachos, D. G. *Langmuir* **2003**, *19*, 4619−4626.
(55) Noh, J. S.; Schwarz, J. A. *J. Colloid Interface Sci.* **1989**, *130*, 157−164.
(56) Santhanam, N.; Conforti, T. A.; Spieker, W.; Regalbuto, J. R. *Catal. Today* **1994**, *21*, 141−156.
(57) Hao, X.; Spieker, W. A.; Regalbuto, J. R. *J. Colloid Interface Sci.* **2003**, *267*, 259−264.
(58) Spieker, W. A.; Regalbuto, J. R. *Chem. Eng. Sci.* **2001**, *56*, 3491−3504.
(59) Marc, S.; Sarah, T.; Latonia, B.; John, R. R.; Jeffrey, T. M. *Nanotechnology* **2005**, *16*, S582.
(60) Chao, K.-J.; Tasi, T. C.; Chen, M.-S.; Wang, I. *J. Chem. Soc., Faraday Trans. 1* **1981**, *77*, 547−555.
(61) Eapen, M. J.; Reddy, K. S. N.; Shiralkar, V. P. *Zeolites* **1994**, *14*, 295−302.
(62) van Dam, H. E.; Kieboom, A. P. G.; van Bekkum, H. *Starch/Staerke* **1986**, *38*, 95−101.
(63) Kuster, B. F. M. *Starch/Staerke* **1990**, *42*, 314−321.